DEVELOPMENTS IN TWO-TIME-SCALE TURBULENCE MODELS APPLIED TO NON-EQUILIBRIUM FLOWS

Tania S. Klein, Tim J. Craft, Hector Iacovides
School of Mechanical, Aerospace and Civil Engineering
The University of Manchester
Oxford Road, Manchester, M13 9PL, UK
tania.klein@postgrad.manchester.ac.uk

ABSTRACT

Multiple-time-scale models have been recently studied by the authors with focus on predicting non-equilibrium flows. Two two-time-scale linear-eddy-viscosity models have been further developed, improved and tested over a wide range of test cases, including simple flows, such as channel flows and zero pressure gradient boundary layers, and more complex flows such as homogeneous shear flows, adverse-pressure-gradient, favourable-pressure-gradient and oscillatory boundary layers, normally strained flows, fully developed ramp up and oscillatory pipe flows and steady backward facing step flows. The two new models performed reasonably well in all test cases, specially when taking into account the inherent limitations of linear-eddy-viscosity schemes.

INTRODUCTION

Non-equilibrium flows are often characterized by the occurrence of sudden changes in the flow such as sudden expansion and/or contraction, sudden changes in the pressure, or rapid time variation of the flow. These flows are quite common in industry and therefore there is a strong interest in their reliable prediction.

It is well known that there is a lag in the response of the turbulence to changes in the mean flow. The energy transfer is best described by the energy cascade process across the turbulent kinetic energy spectrum which is thus characterized by a range of time and length scales. Therefore single-time-scale turbulence models, which comprise most of the Reynolds Averaged Navier Stokes (RANS) models, and which assume that a single length or time scale is able to characterize a flow, are less likely to predict such non-equilibrium flows correctly.

Two-time-scale turbulence models have thus arisen as an attempt to take into account some features of the turbulent kinetic energy spectrum within the RANS modelling framework, and thus to improve the prediction of non-equilibrium flows.

Two-time-scale turbulence models based on the idea of Hanjalic *et al.* (1980) split the turbulent kinetic energy spectrum into three zones: production, transfer and dissipation zones. The variable k_P denotes the kinetic energy contained in the large-scale turbulent eddies in the production zone which is transfered at a rate ε_P to the transfer zone where the smaller turbulent eddies contain energy denoted by the variable k_T. The turbulent kinetic energy is then transfered to the dissipation zone at a rate ε_T where it is immediately dissipated into heat and therefore none of the total turbulent kinetic energy is stored in this zone. The turbulent kinetic energy dissipation rate ε, usually used in single-time-scale models, is then equivalent to ε_T. If using this decomposition within a linear eddy viscosity modelling approach, transport equations for each of the partition variables (k_P, k_T, ε_P and ε_T) must be solved.

In this work two two-time-scale models based on the above framework will be presented. They are a result of further improvement in the work presented by Klein *et al.* (2010) in order to comply with some physical constraints associated with different parts of the turbulent kinetic energy spectrum.

TURBULENCE MODELLING

The two two-time-scale models developed are based on linear eddy-viscosity formulations, however the eddy viscosity was set to vary with the mean dimensionless strain rate $\eta = \frac{k}{\varepsilon_T} max(S,W)$, as is sometimes done in non-linear-eddy-viscosity approaches. In the above η expression, $S = \frac{S_{ij}S_{ij}}{2}$, $W = \frac{W_{ij}W_{ij}}{2}$, $S_{ij} = \left(\frac{\partial U_i}{\partial x_j} + \frac{\partial U_j}{\partial x_i}\right)$ and $W_{ij} = \left(\frac{\partial U_i}{\partial x_j} - \frac{\partial U_j}{\partial x_i}\right)$. The main difference between the two models proposed is the eddy-viscosity formulation, where the use of different time scales was explored. As a consequence of this difference, slightly different terms are included in the modelled transport equations for the turbulent quantities.

The transport equations for the partition variables, equations 1 to 4, are presented below and will be used as reference to comment on the new models developed.

$$\frac{Dk_P}{Dt} = P_k - \varepsilon_P + \frac{\partial}{\partial x_j}\left[\left(\nu + \frac{\nu_t}{\sigma_k}\right)\frac{\partial k_P}{\partial x_j}\right] \qquad (1)$$

$$\frac{Dk_T}{Dt} = \varepsilon_P - \varepsilon_T + \frac{\partial}{\partial x_j}\left[\left(\nu + \frac{\nu_t}{\sigma_k}\right)\frac{\partial k_T}{\partial x_j}\right] \quad (2)$$

$$\frac{D\varepsilon_P}{Dt} = C_{P1}P_k\frac{\varepsilon_P}{k_P} - C_{P2}\frac{\varepsilon_P^2}{k_P} + \frac{\partial}{\partial x_j}\left[\left(\nu + \frac{\nu_t}{\sigma_{\varepsilon_P}}\right)\frac{\partial \varepsilon_P}{\partial x_j}\right] + C'_{P1}k_P\frac{\partial U_l}{\partial x_m}\frac{\partial U_i}{\partial x_j}\varepsilon_{lmk}\varepsilon_{ijk} \quad (3)$$

$$\frac{D\varepsilon_T}{Dt} = C_{T1}\frac{\varepsilon_P\varepsilon_T}{k_T} - C_{T2}\frac{\varepsilon_T^2}{k_T} + \frac{\partial}{\partial x_j}\left[\left(\nu + \frac{\nu_t}{\sigma_{\varepsilon_T}}\right)\frac{\partial \varepsilon_T}{\partial x_j}\right] \quad (4)$$

The coefficients and functions applied in the models were defined through asymptotic analysis of homogeneous shear flows, decaying grid turbulence and local equilibrium boundary layers. A further constraint applied in this latter flow was to ensure that the ratio $\frac{k_P}{k_T}$ should be greater than 3, in order to ensure that the ratio of length and time scales between the production and transfer zones was greater than unity, as one might physically expect to be the case.

NT1 Model

The NT1 model was developed by using the same general expression for the eddy-viscosity as that proposed by Hanjalic *et al.* (1980), $\nu_t = c_\mu \frac{kk_P}{\varepsilon_P}$. However, instead of a constant, $c_\mu = min[0.115, 0.023 + 0.25exp(-0.3\eta)]$ so that it varies with the dimensionless shear. The coefficient 0.115 represents the value c_μ is expected to assume in equilibrium boundary layers. The time-scale used in this formulation of ν_t is based on the large eddies $\frac{k_P}{\varepsilon_P}$.

The last term in equation 3 was identified to cause instabilities in the homogeneous shear flows. Moreover, it was found that the model would return best results in these flows when $C'_{P1} = 0$. It was also found to be beneficial to make the coefficient C_{P1}, also in equation 3, to vary as a function of the ratio $\frac{k_P}{k_T}$ in order to improve prediction of homogeneous low shear cases. Its final form adopted is $C_{P1} = 1.4912 + 2.5min(0, \frac{k_P}{k_T} - 3.6)/(\frac{k_P}{k_T} + 3.6)$, where 3.6 is the expected value for the ratio $\frac{k_P}{k_T}$ in equilibrium boundary layers.

The remaining coefficients were kept as constants, even C_{T1} which varies with $\frac{\varepsilon_P}{\varepsilon_T}$ in Hanjalic *et al.* (1980), and are presented in Table 1.

NT2 Model

The NT2 model was developed in order to test the eddy-viscosity as a function of the total time scale, just as used in single-time-scale models: $\nu_t = c_\mu \frac{k^2}{\varepsilon_T}$. Again, c_μ was taken to vary with η and assumed the form: $c_\mu = min(0.09, 0.0117 + 0.22exp(-0.31\eta)$. The value expected for c_μ in equilibrium boundary layers is the same as that used in single-time-scale models.

Again, C_{P1} in equation 3 was made to vary with the ratio $\frac{k_P}{k_T}$, assuming the form $C_{P1} = 1.5697 + 2.5min(0, \frac{k_P}{k_T} - 3.7)/(\frac{k_P}{k_T} + 3.7)$, where 3.7 is the expected value for the ratio $\frac{k_P}{k_T}$ in equilibrium boundary layers. However, in this model, a small contribution of the term which includes the coefficient C'_{P1} in equation 3 was found beneficial to improve prediction in the homogeneous low shear cases. This small contribution did not cause the instabilities found in the model of Hanjalic *et al.* (1980).

The coefficient C_{T1} was kept as a function of the ratio $\frac{\varepsilon_P}{\varepsilon_T}$ as in Hanjalic *et al.* (1980) which effectively implies a different source term in equation 4 which then becomes:

$$\frac{D\varepsilon_T}{Dt} = C_{T1}\frac{\varepsilon_P^2}{k_T} - C_{T2}\frac{\varepsilon_T^2}{k_T} + \frac{\partial}{\partial x_j}\left[\left(\nu + \frac{\nu_t}{\sigma_{\varepsilon_T}}\right)\frac{\partial \varepsilon_T}{\partial x_j}\right] \quad (5)$$

Both NT1 and NT2 models use a constant for the coefficient C_{P2}, which comes directly from decaying grid turbulence analysis, just as is done in single-time-scale models. It may be noted that neither the NT1 or the NT2 model follows exactly the general form of the model proposed by Hanjalic *et al.* (1980), but modifications were proposed in order to improve prediction of homogeneous shear flows and at the same time to comply with the asymptotic analysis of the various flows noted above.

Table 1. Constant coefficients for the NT1 and NT2 models

Coefficient	NT1 model	NT2 model
C_{P2}	1.8	1.8
C'_{P1}	0	-0.005
σ_{ε_P}	1.4202	1.6664
C_{T1}	1.6	1.0
C_{T2}	1.7	1.1
σ_{ε_T}	1.2181	1.1922
σ_k	1.0	1.0

TEST CASES

These most recent versions of the two two-scale-models, outlined above, have been tested over a wide variety of flows.

Simple flows such as channel flows and zero pressure gradient boundary layers were tested in order to ensure that the models provide reasonable results even in such simple cases. Results showing the performance of the new models in these cases will not be presented here since they are not the main focus of prediction.

More complex test cases such as homogeneous shear flows, adverse-pressure-gradient, favourable-pressure-gradient and oscillatory boundary layers, normally strained flows, fully developed ramp up and oscillatory pipe flows and

steady backward facing step flows were also used to assess the performance of the new models. A sample of the results obtained in these test cases will be shown here within the results.

In order to simulate the test cases mentioned above, the in-house finite volume fully collocated grid CFD code STREAM, described in Lien & Leschziner (1994), was used. Besides DNS data and/or experiments, the performance of the new models will be compared with three other turbulence models: the linear-eddy-viscosity standard $k-\varepsilon$ model, the Reynolds stresses transport model SSG of Speziale *et al.* (1991) and the two-time-scale model of Hanjalic *et al.* (1980) which will be referred to as the HLS model.

All five models tested here are high Reynolds number formulations which means they need to be used together with wall functions. The wall function used here is the log-law based formulation proposed by Chieng & Launder (1980). Adaptations were made in order to use it with the two-time-scale models: the regular wall function treatment was applied to k_P and ε_T, and, consistent with the assumption of local equilibrium boundary layer conditions, ε_P was set equal to ε_T and the ratio $\frac{k_P}{k_T}$ at the near wall cell was set as 2 for the two-time-scale model of Hanjalic *et al.* (1980) and as 3.6 and 3.7 for the NT1 and NT2 schemes respectively, since these are the values predicted by these models in such an equilibrium boundary layer.

RESULTS

The performance of the new NT1 and NT2 linear-eddy-viscosity two-time-scale models will be assessed in a range of challenging cases below.

Homogeneous Shear Flows

Homogeneous shear flows, consisting of a constant velocity gradient being applied to quasi-isotropic developing flows, have been tested over a range of dimensionless shear values, $\frac{k}{\varepsilon}\frac{dU}{dy}$, from about 1 to 30. Most RANS turbulence models perform reasonably well in low shear cases, however, as this parameter is increased, they are not able to follow the development of turbulent quantities. In Figures 1, 2 and 3 the performance of the new models in predicting the evolution in time of the turbulent kinetic energy can be seen for low, moderate and high shear cases respectively. It is noticeable that the new models perform quite satisfactorily, bringing clear improvements over the $k-\varepsilon$ and the HLS models, even compared to the much more complex SSG model. Although only the prediction of the turbulent kinetic energy is being presented here, the development of the eddy dissipation rate and the Reynolds shear stress also show similar results.

Adverse Pressure Gradient Boundary Layers

This case consists of a boundary layer where the freestream pressure increases in the streamwise direction. Consequently, the freestream velocity decreases and therefore this case is also known as decelerating flow. The pressure can increase either due to the geometry of the flow or by an imposed pressure gradient. Three different adverse pressure gradient boundary layers have been tested in this work, the highest Reynolds number case from Marusic & Perry (1995) being chosen to be shown here. In Figure 4 one can see the

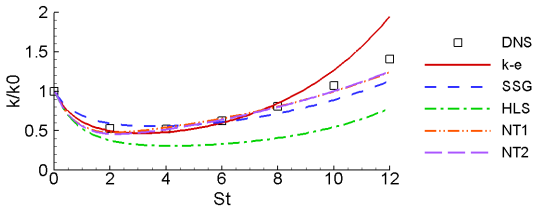

Figure 1. Prediction of the turbulent kinetic energy in the lowest shear case of Rogers & Moin (1987)

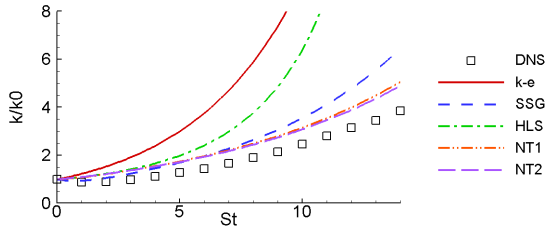

Figure 2. Prediction of the turbulent kinetic energy in the moderate shear case of Matsumoto *et al.* (1991)

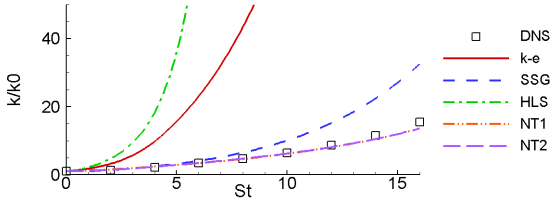

Figure 3. Prediction of the turbulent kinetic energy in the high shear case of Lee *et al.* (1990)

prediction of the Reynolds shear stress at the last measurement position where the pressure gradient is stronger than in any other position downstream. Again, one can see very reasonable prediction from the new two-time-scale models. The performance of the new models are not so close to the experimental data when predicting the the mean velocity and turbulent kinetic energy profiles, however none of the models herein considered were able to provide clearly better results, since all models fail to follow the subtle changes downstream presented by the experimental data.

Favourable Pressure Grad. Boundary Layers

This case consists of a boundary layer where the freestream pressure decreases in the streamwise direction. Consequently, the freestream velocity increases and therefore this case is also known as accelerating flow. However, in this case, the flow reaches a self-similar state. The DNS of Spalart (1986) was used to assess the performance of the models. In Figure 5 one can see the prediction of the turbulent kinetic energy in the lowest acceleration case. The NT1 and NT2 models perform reasonable well and this comment can be extended

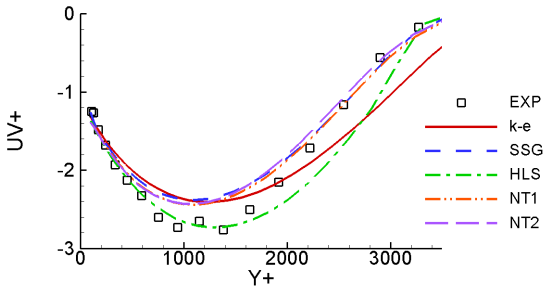

Figure 4. Prediction of the turbulent shear stress at the last measurement position in the highest Reynolds number case of Marusic & Perry (1995).

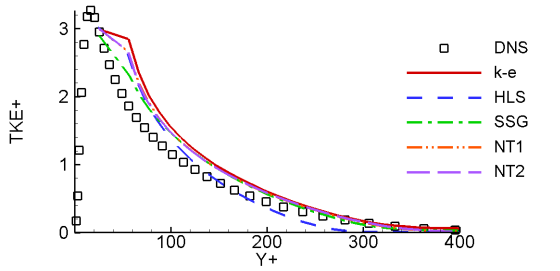

Figure 5. Prediction of the turbulent kinetic energy in the lowest acceleration ($K = 1.5 \times 10^{-6}$) case of Spalart (1986).

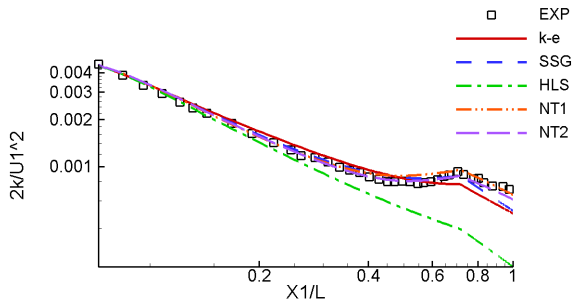

Figure 6. Prediction of the turbulent kinetic energy in the normally strained case of Tucker & Reynolds (1968)

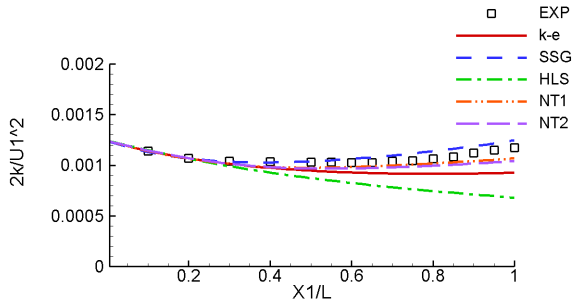

Figure 7. Prediction of the turbulent kinetic energy in the pure plane strained case of Gence & Mathieu (1979)

to the prediction of the velocity profile and the other turbulent quantities. Although not shown here, the new models also perform well for the two other acceleration cases reported by Spalart (1986) with acceleration parameter $K = 2.5 \times 10^{-6}$ and $K = 2.75 \times 10^{-6}$, K being defined as $\frac{\nu}{U_\infty^2}\frac{dU_\infty}{dx}$ where U_∞ is the freestream velocity.

Normally Strained

This case consists of applying normal straining to a flow, causing sudden expansion and contraction to occur in perpendicular directions. Two cases were chosen in order to show the capabilities in improving prediction of the new models. The first case is the laterally distorting tunnel case of Tucker & Reynolds (1968) where the straining starts at x1/L = 0.14 and is interrupted at x1/L = 0.71, where L is the length of the test section, and the second case is the pure plane strain in an elliptical distorting duct of Gence & Mathieu (1979). Both cases were set by fixing the normal straining and simulating the centreline of the flow. The prediction of the turbulent kinetic energy for the first and second cases are presented in Figures 6 and 7 respectively. The NT1 and NT2 models perform as well as the SSG model and clearly better than the $k-\varepsilon$ and HLS models.

Fully Developed Oscillatory Pipe Flow

Both oscillatory boundary layer and fully developed oscillatory pipe flows have been used as test cases. The former was well predicted by all models, thus not representing a challenging case and therefore is not presented here. Oscillatory pipe flows were shown to be more sensitive to the imposed oscillation frequency. At low frequencies, the flow experiences a series of steady state situations while at high frequencies, frozen turbulence is observed and the oscillatory effects are mostly confined in the viscous sublayer. It is then in the intermediate frequency range where more non-equilibrium features are found and where the performance of the turbulence models vary more. The T3RE14A20 case of He & Jackson (2009), which falls into this intermediate frequency range, was thus used to assess the performance of the two new models. The prediction of the amplitude and phase shift of oscillation of the Reynolds shear stress is presented in Figures 8 and 9. One may notice that although the new NT1 and NT2 models do not provide the best agreement with the experimental data, they do provide reasonable predictions and this was also found to be the case over a range of oscillation frequencies.

Fully Developed Ramp Up Pipe Flow

This case consists of a fully developed pipe flow where the bulk velocity is linearly increased in time, thus characterizing a ramp function. Non-equilibrium effects are here present because the turbulence shows a lag in its response to the increase in the mean velocity. The experiments of He & Jackson (2000) were used to assess the performance of the models in this test case. One can see in Figures 10 and 11, showing the streamwise development of turbulent kinetic energy and shear stress, that both new models perform reason-

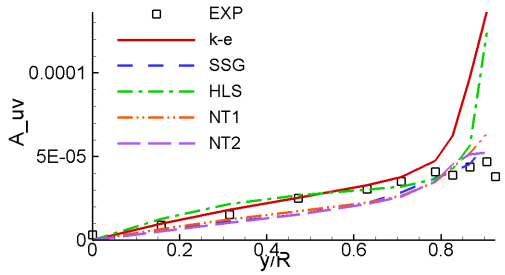

Figure 8. Prediction of the amplitude of oscillation of the Reynolds shear stress in the T3RE14A20 case of He & Jackson (2009)

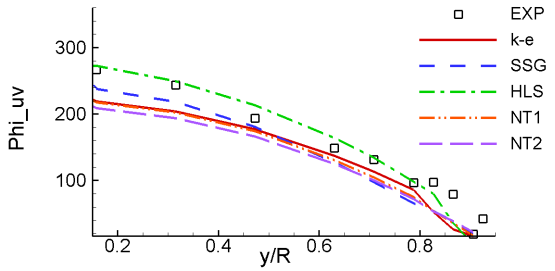

Figure 9. Prediction of the phase shift of oscillation of the Reynolds shear stress in the T3RE14A20 case of He & Jackson (2009)

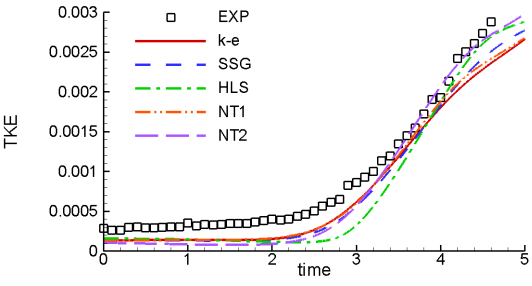

Figure 10. Prediction of the turbulent kinetic energy in the fully developed ramp up pipe flow of He & Jackson (2000) at $y/R = 0.47$

ably well and that they do present improvements compared to the HLS model regarding the prediction of the moment when the turbulence responds to the change in mean velocity.

Backward Facing Step Flow

In a backward facing step flow, the flow faces a sudden expansion due to a step in the original channel and therefore non-equilibrium features are present. The sudden step generates curved streamlines and recirculation zones which are confined between the step and the reattachment point, which thus becomes a key parameter in such flows. The experiment

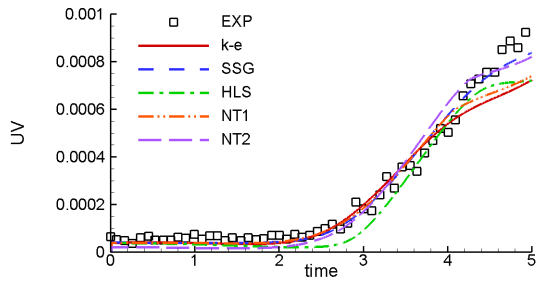

Figure 11. Prediction of the Reynolds shear stress in the fully developed ramp up pipe flow of He & Jackson (2000) at $y/R = 0.47$

studied here is the steady case of Chun & Sung (1996) which was characterized as a 2-D flow with an expansion ratio of 1.5. The prediction of the reattachment point by each turbulence model is presented in Table 2 and the velocity profile just before the step and in five positions downstream of the step is presented in Figure 12, where H is the step height.

Starting by commenting on the prediction of the reattachment points, one can see in Table 2 that none of the models captured correctly the reattachment point, the three existing models tending to underpredict it and the two new models tending to overpredict it. The term associated with the coefficient C'_{P1} in equation 3 was identified as being responsible for the big underprediction of the reattachment point by the HLS model together with the imbalance of this model's coefficients with regard to the asymptotic analysis of equilibrium boundary layers. The deviation between predicted and measured reattachment lengths for the new NT1 and NT2 models is similar to those of the other models used for comparison, even much more complex models such as the SSG.

With regard to the prediction of the velocity profiles, Figure 12, the standard $k-\varepsilon$ model apparently provides the best agreement with the experimental data. The reason is that the $k-\varepsilon$ predicts an earlier reattachment, which gives the model enough time to recover its regular channel profile. On the other hand, the SSG model, which also underpredicted the reattachment length, returns velocity profiles similar to those of the new NT1 and NT2 models. It is more straightforward to understand the profiles presented by the new models since they overpredicted the reattachment point, however the profiles provided by the SSG model may be explained by a rather slow recovery to the fully-developed channel flow profiles. The profiles produced by the HLS model are consistent with this model's strong underprediction of the reattachment point.

CONCLUDING REMARKS

Two two-time-scale models were presented and their performance in a wide variety of non-equilibrium flows has been assessed. The models returned overall good prediction in all flows, specially in the homogeneous shear flows and normally strained flows, despite the inherent limitations of the linear eddy-viscosity approximation.

Adjustments in the models are still required and are in progress in other to improve prediction in the oscillatory pipe

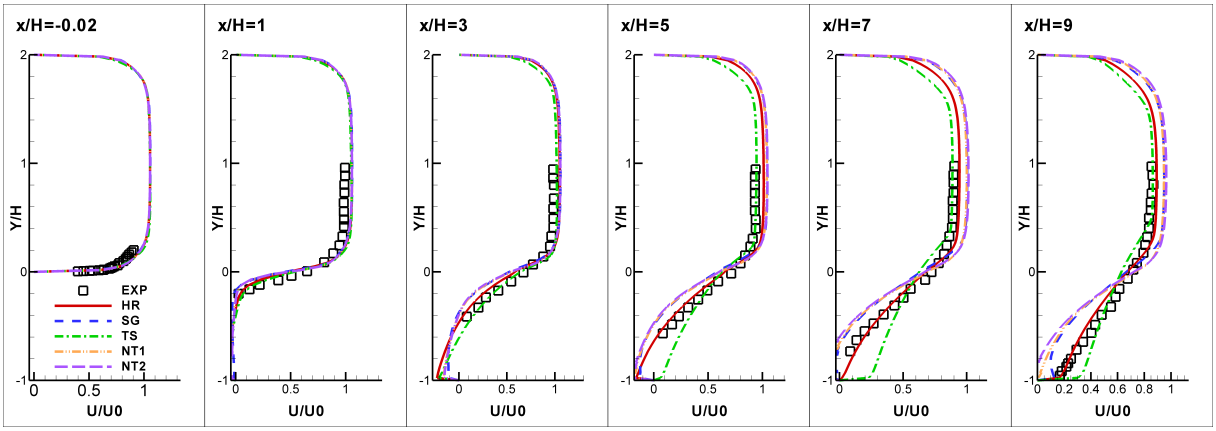

Figure 12. Prediction of the velocity profile in the steady backward facing step case of Chun & Sung (1996)

Table 2. Prediction of the reattachment point in the steady backward facing step case

Model/Case	Reattachment point (x/H)	% Error
Experiments	7.8	-
$k-\varepsilon$	6.6	−15.8
HLS	4.2	−46.4
SSG	7.0	−10.7
NT1	8.9	14.0
NT2	9.5	21.8

flows and backward facing step flows. The unsteady backward facing step cases of Chun & Sung (1996) are also being studied in order to provide a broader view of the performance of the new models.

ACKNOWLEDGEMENTS

The authors acknowledge the support of the School of MACE for the ORS scholarship and CNPq, National Council for Scientific and Technological Development - Brazil, for the PhD scholarship.

REFERENCES

Chieng, C. C. & Launder, B. E. 1980 On the calculation of turbulent heat transport downstream from an abrupt pipe expansion. *Numerical Heat Transfer, Part A: Applications* **3**, 189–207.

Chun, K. B. & Sung, H. J. 1996 Control of turbulent separated flow over a backward-facing step by local forcing. *Experiments in Fluids* **21**, 417–426.

Gence, J. N. & Mathieu, J. 1979 On the application of successive plane strains to grid-generated turbulence. *J. Fluid Mech.* **93**, 501–513.

Hanjalic, K., Launder, B. E. & Schiestel, R. 1980 Multiple-time-scale concepts in turbulent transport modelling. In *Turbulent Shear Flows 2*.

He, S. & Jackson, J. D. 2000 A study of turbulence under conditions of transient flow in a pipe. *J . Fluid Mech.* **408**, 1–38.

He, S. & Jackson, J. D. 2009 An experimental study of pulsating turbulent flow in a pipe. *European Journal of Mechanics B/Fluids* **28**, 309320.

Klein, T. S., Craft, T. J. & Iacovides, H. 2010 Two-time-scale turbulence models for non-equilibrium flows. In *8th international symposium on engineering turbulence modelling and measurements*. Marseille, France.

Lee, M. J., Kim, J. & Moin, P. 1990 Structure of turbulence at high shear rate. *J. Fluid Mech* **216**, 561–583.

Lien, F. S. & Leschziner, M. A. 1994 A general non-orthogonal collocated finite volume algorithm for turbulent flow at all speeds incorporating second-moment turbulence-transport closure, part 1: Computational implementation. *Computer Methods in Applied Mechanics and Engineering* **114**, 123–148.

Marusic, I. & Perry, A. E. 1995 A wall-wake model for the turbulence structure of boundary layers. part 2. further experimental support. *J. Fluid Mech* **298**, 389–407.

Matsumoto, A., Nagano, Y. & Tsuji, T. 1991 Direct numerical simulation of homogeneous turbulent shear flow. 5th Symposium on Computational Fluid Dynamics, Tokyo.

Rogers, M. M. & Moin, P. 1987 The structure of the vorticity field in homogeneous turbulent flows. *J. Fluid Mech* **176**, 33–66.

Spalart, P. R. 1986 Numerical study of sink-flow boundary layers. *J. Fluid Mech* **172**, 307–328.

Speziale, C. G., Sarkar, S. & Gatski, T. B. 1991 Modelling the pressure-strain correlation of turbulence: an invariant dynamical systems approach. *J. Fluid Mech.* **227**, 245–272.

Tucker, H. J. & Reynolds, A. J. 1968 The distortion of turbulence by irrotational plane strain. *J . Fluid Mech.* **32**, 657–673.